



## Supercapacitors as redox mediators for decoupled water splitting

Mingrui Guo<sup>a,1,\*</sup>, Jing Zhan<sup>b,1</sup>, Zekun Wang<sup>b</sup>, Xiaorui Wang<sup>c</sup>, Zhang Dai<sup>b</sup>, Ting Wang<sup>b,\*</sup>

<sup>a</sup> College of Chemistry and Chemical Engineering, Institute for Sustainable Energy and Resources, Qingdao University, Qingdao 266071, China

<sup>b</sup> National Engineering Research Center for Colloidal Materials, School of Chemistry and Chemical Engineering, Shandong University, Ji'nan 250100, China

<sup>c</sup> Shandong Shengtong Optical Materials Technology Co., Ltd., Dongying 257500, China



### ARTICLE INFO

#### Article history:

Received 13 July 2022

Accepted 26 July 2022

Available online 28 July 2022

#### Keywords:

Decoupled water splitting

Redox mediators

Supercapacitors

High current density

Ultralong cycle-life

### ABSTRACT

With the help of the redox mediator, decoupled water-splitting allows O<sub>2</sub> and H<sub>2</sub> to be produced at different times, at different rates, and even in different cells, which promotes both the operation safety and the utilization of renewable power sources. However, the current densities and stabilities of these redox mediators are commonly low, which require further improvements for practical applications. Here, we propose to use supercapacitors as solid state redox mediators for decoupled water splitting. For demonstration, Na<sub>0.5</sub>MnO<sub>2</sub> (pseudocapacitor) and active carbon (double layer capacitor), are both used as the redox mediator. These supercapacitors show superior current density (1 A/cm<sup>2</sup>) and ultralong cycle-life (8000 cycles) compared with commonly investigated battery-based mediators (NiOOH/Ni(OH)<sub>2</sub>). Our research proves supercapacitors can be used as redox relay with high current density and stability, which may bring new insights in the design of decoupled water splitting systems.

© 2022 Published by Elsevier B.V. on behalf of Chinese Chemical Society and Institute of Materia Medica, Chinese Academy of Medical Sciences.

Hydrogen with high energy density by weight is highly promising to replace the fossil fuels and reduce CO<sub>2</sub> emissions [1–7]. Electrolytic water splitting, driven by renewable energy sources such as solar and wind, represents an important way for green hydrogen production [8–10]. Despite the rapid development of a variety of novel electrocatalyst for hydrogen evolution reaction (HER) [11,12] and oxygen evolution reaction (OER) [13,14], an equally important issue is to design new water splitting systems to overcome some critical challenges confronted by conventional water electrolysis, such as gas mixing issues and the incompatibility with fluctuated green energies [15–18].

To address these issues, one interesting topic that has been proposed recently is to decouple the water splitting in space and/or in time [19–21]. Redox mediators are commonly used to achieve the HER/OER decoupling, which bring extra reactions pairing with the HER and OER. As such, a one-step reaction is decoupled into a two-step process. Up to now, a variety of agents have been developed as redox mediators [22–24], including soluble ones, such as polyoxometalates [25], and solid-state redox mediators [26–28], such as NiOOH/Ni(OH)<sub>2</sub> [26]. A few nice review papers summarized the developments of different types of redox mediators [29,30]. Despite the rapid development of decoupled water splitting, there

are several constraints that prohibit their practical implementation [31,32]. One problem is that the long-term stability of the redox agents upon repeated redox cycling remains unproven, another problem is that the current density of reported decoupled water splitting systems is generally low (the number of cycles and the current density tested for typical redox mediators are provided in Table S1 in Supporting information). Redox mediators with long cycle life and high current density still require further investigation.

With the development of energy storage technologies, supercapacitors such as electric double layer capacitors and pseudocapacitors, are thoroughly investigated and their applications well explored [33–35]. In general, the key function for the redox mediator in decoupled water splitting is “decoupling”, which means robust, rapid redox reactions to decouple the HER and OER, and the energy storage capacity is not crucial. As a result, supercapacitors [36–38] with high, tunable power rates (specific power 500–10000 W/kg), rapid charge/discharge speed (seconds to minutes), large Coulombic efficiency (85%–98%) and ultralong cycle-life (above 500000) may be more suitable to work as solid state redox mediators for decoupled water splitting compared with the widely investigated battery-based redox relay, such as NiOOH (Fig. S1 in Supporting information).

Here, we propose to use supercapacitors as solid state redox mediators. As a simplified model (Fig. 1a), in an electrochemical cell using basic electrolytes, a bifunctional (HER and OER) electrode is used as the gas evolution electrode for H<sub>2</sub> and O<sub>2</sub> generation,

\* Corresponding authors.

E-mail addresses: [gmrqdx@qdu.edu.cn](mailto:gmrqdx@qdu.edu.cn) (M. Guo), [t54wang@sdu.edu.cn](mailto:t54wang@sdu.edu.cn) (T. Wang).

<sup>1</sup> These authors contributed equally to this work.

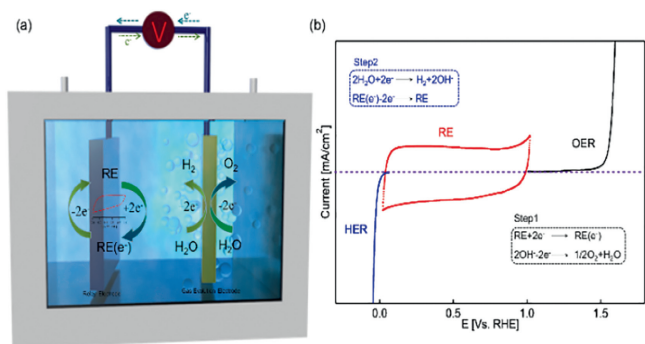


**Fig. 1.** (a) Schematic illustration of decoupled water splitting using a bifunctional (HER/OER) electrode and supercapacitor-type mediators. (b) Cyclic voltammograms (CV) curves of the AC relay electrode (red line), the linear sweep voltammetric (LSV) curves of the NiFe-LDH@Pt-coated Ti-mesh for the HER (blue line), the OER (black line) in 1 mol/L NaOH.

and supercapacitors used as the relay electrode [39]. As shown in Fig. 1b, in step 1, the HER process is coupled with the charging of the supercapacitor. In step 2, by reversing the current flow, OER process is coupled with the discharging of the supercapacitor. For demonstration, a typical double layer capacitor, active carbon (AC), and a typical pseudocapacitor,  $\text{Na}_{0.5}\text{MnO}_2$ , are both used as the relay electrode for decoupled water splitting.  $\text{Na}_{0.5}\text{MnO}_2$  electrode was selected as another type of the pseudocapacitor electrode owing to their proper redox positions, low cost, high specific capacitance and long cycle life. For both the active carbon and  $\text{Na}_{0.5}\text{MnO}_2$  as the redox mediator, the decoupling processes show rapid gas evolution rate owing to the rapid charging/discharging of the supercapacitor, both electrodes show high Coulombic efficiency, the decoupling efficiency is tunable and directly related to the gas evolution speed. Meanwhile, both electrodes show ultra-long cycle-life (8000 cycles in 223 h for AC and 8000 cycles in 223 h for  $\text{Na}_{0.5}\text{MnO}_2$ ). These supercapacitor based relay mediator show much better performance compared with the traditionally used battery electrodes. Our research may bring new insights in the selection of redox mediators for decoupled water splitting.

The configuration of as-designed cell for decoupled water splitting is shown in Fig. S2 (Supporting information), and Ti foil with deposited Pt and hydrothermally grown Ni/Fe LDH (Fig. S3 in Supporting information) is used as the gas evolution electrode (GEE). The preparation of the gas evolution electrode is shown in Supporting information. The surface morphology and structure of the NiFe-LDH@Pt-coated Ti-mesh is confirmed by the SEM images and XRD pattern (Figs. S4 and S5 in Supporting information). The GEE showed both high HER and high OER activities, which is presented in Fig. S6 (Supporting information).

The details for the preparation of the AC electrode is provided in Supporting information. The structure and surface morphology of as-prepared AC relay is confirmed by XRD and SEM (Fig. S7 in Supporting information). With active carbon as the relay, the mechanism is shown in Fig. 2a, while the discharging of the AC electrode,  $\text{O}_2$  is produced on the GEE by an anodic oxidation of the  $\text{OH}^-$ . By reversing the current polarity,  $\text{H}_2$  is produced on the GEE while the AC relay charged. The cyclic voltammogram (CV) curve of the AC electrode tested at a scan rate of 1 mV/s using Ag/AgCl as the reference electrode is shown in Fig. 2b. The charging/discharging processes are symmetric and there is no obvious redox peaks observed in the curve, which is consistent with the double layer capacitor nature of the AC electrode in the HER and OER processes. For the charging/discharging processes of the AC relay electrode, with a constant current flow, the capacity of the electrode is 1.1 F/cm<sup>2</sup> (Fig. 2c), which is typical for double layer supercapacitors. The charging/discharging performance of AC elec-

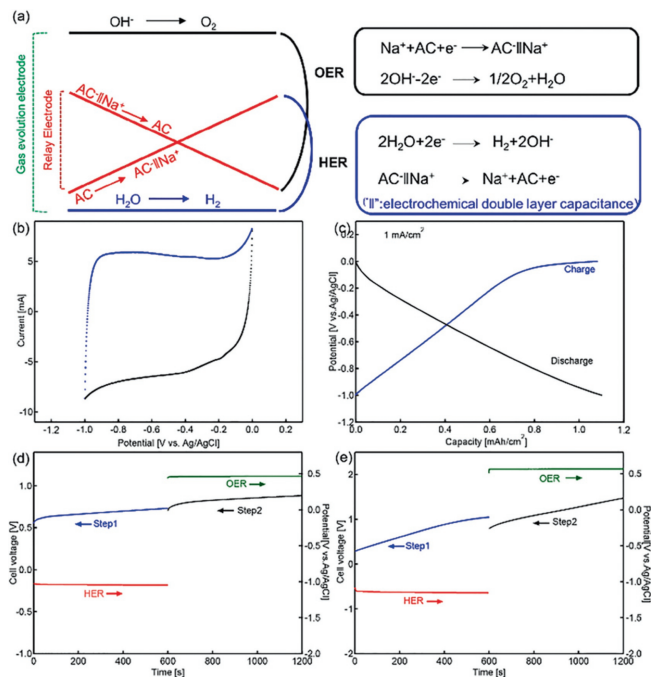


**Fig. 2.** (a) Illustration of the mechanism for the decoupled water splitting using AC as relay. (b) CV curve of the AC electrode. (c) Charge/discharge with a current density of 1 mA/cm<sup>2</sup> of AC in 1 mol/L NaOH. (d, e) Chronopotentiometry curves (Cell voltage vs. time) for the H<sub>2</sub>/O<sub>2</sub> production steps (blue/black line) and the chronopotentiometry data (potential vs. time) of bifunctional (HER/OER) electrode (red/green line) at a current of 10 mA and 100 mA respectively.

trode tested with different current flow is shown in Fig. S8 (Supporting information).

Unlike common redox mediators, with the supercapacitors as the relay, the potential for the decoupled reaction under a fixed current is not a constant. As shown in Fig. 2d, at a constant current of 10 mA, the as-designed cell requires a cell voltage of 0.68 V for the HER step and 0.834 V for the OER step. With current increased to 100 mA (Fig. 2e), the as-designed cell requires a cell voltage of 0.75 V for the HER step and 1.18 V for the OER step. For decoupled water splitting, the decoupling efficiency (DE) is commonly calculated by comparison of the operating voltage between the two-step water splitting and the one-step process without the relay electrodes. Based on a comparison of their operating voltage, the DEs of the decoupled water splitting using the AC relay at current of 10 mA and 100 mA were calculated to be 99% and 90%. Meanwhile, the overall energy conversion efficiency using the AC relay at current of 10 mA and 100 mA were calculated to be 98% and 78%, which indicate ultrasmall energy loss with low current flow (Fig. S9 in Supporting information).

The long-term stability of the AC relay electrode under constant current (200 mA, 100 s for 1 cycle) is investigated. As shown in Figs. 3a-c, the first 10 cycle, middle 10 cycles and the last 10 cycles are enlarged. No obvious performance decay is observed, which confirms the high stability of the relay electrode. At a cell current of 200 mA, the two-step water splitting process can be reversibly cycled for 8000 rounds in 223 h without noticeable decay (Fig. 3d).

The preparation of the  $\text{Na}_{0.5}\text{MnO}_2$  relay electrode follows previous reports. With  $\text{Na}_{0.5}\text{MnO}_2$  (a typical pseudocapacitor) as the relay for decoupling, the mechanism and properties are shown in Supporting information, while the discharging of the  $\text{Na}_{0.5}\text{MnO}_2$  ( $\text{Mn}^{4+}$  reduced to  $\text{Mn}^{3+}$ ),  $\text{O}_2$  is produced on the GEE by an anodic oxidation of the  $\text{OH}^-$ . By reversing the current polarity,  $\text{H}_2$  is produced on the GEE while the  $\text{Na}_{0.5}\text{MnO}_2$  relay charged (Fig. S10 in Supporting information). In operation, the as-designed cell requires

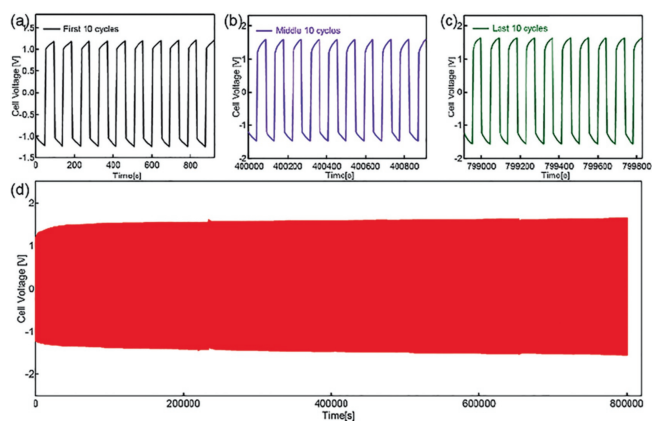


**Fig. 3.** Chronopotentiometry curve (cell voltage as a function of time) for the decoupled water splitting using AC as relay with step time of 50 s at a constant current of 200 mA: (a) The first ten cycles; (b) the middle ten cycles; (c) the last ten cycles. (d) Cycle stability of the  $\text{H}_2/\text{O}_2$  generation cycle during 800,000 s.

a cell voltage of 0.514 V for the OER step and 1.15 V for the HER step at 10 mA/cm<sup>2</sup>. The decoupled water splitting with  $\text{Na}_{0.5}\text{MnO}_2$  relay electrode shows the same high-efficiency and cycle stability (8000 rounds, Fig. S11 in Supporting information), which may be due to the high surface reversible cycling capacity of pseudocapacitance.

The supercapacitors can achieve rapid charge/discharge with large current flow compared with common battery based electrodes, owing to the capacitive ion storage mechanism. With supercapacitors as relay, such a property may promote rapid hydrogen production with high current flow in the decoupled water splitting process. As shown in Fig. 4a, with AC as the relay electrode, at a current density of 1 A/cm<sup>2</sup>, a potential of 2.54 V is required for the HER process and 2.43 V for the OER process. Meanwhile, under different current density (500 mA, 800 mA), the system show stable performance (Fig. S12 in Supporting information), which means the supercapacitors can be used as relay for decoupled water splitting using unstable power supplies.

Meanwhile, large-area AC electrodes ( $10 \times 10 \text{ cm}^2$ ) and GEE electrodes ( $10 \times 10 \text{ cm}^2$ ) were assembled into a decoupling electrolysis device (Fig. 4b and Fig. S13 in Supporting information). The two step  $\text{H}_2/\text{O}_2$  production processes are visualized as shown in Video in Supporting information. Drainage method was used to quantify the substep production of  $\text{H}_2/\text{O}_2$  over a certain period of time and was visualized (Video in Supporting information). In such a device, the decoupling can be achieved using different current flow, as an example, in the first step, low current density (1 A) (with the AC electrode discharge) was used to produce oxygen. In the second step, a large current (10 A) was used to rapidly produce large amount of high-purity hydrogen. Such a strategy may help to produce high-purity hydrogen within a short time. Figs. 4c and d were HER/OER process voltage over time curve. The calculated Faradaic efficiency for the hydrogen production was close to 100%.

In the device, the  $\text{H}_2$  evolution and  $\text{O}_2$  evolution were decoupled in time, and gas chromatographs (GCs) were used to detect the purity of the produced hydrogen and oxygen. The GC data which was obtained during the electrolysis process and the corresponding timing potential data were shown in Fig. S14 (Supporting information). The results clearly showed that the separation process produces only hydrogen and without oxygen. At 100 mA current, with an operating time of 90 min and  $\text{H}_2$  gas production of 2.79 mmol, the Faraday efficiency of hydrogen was calculated to be about 100%.

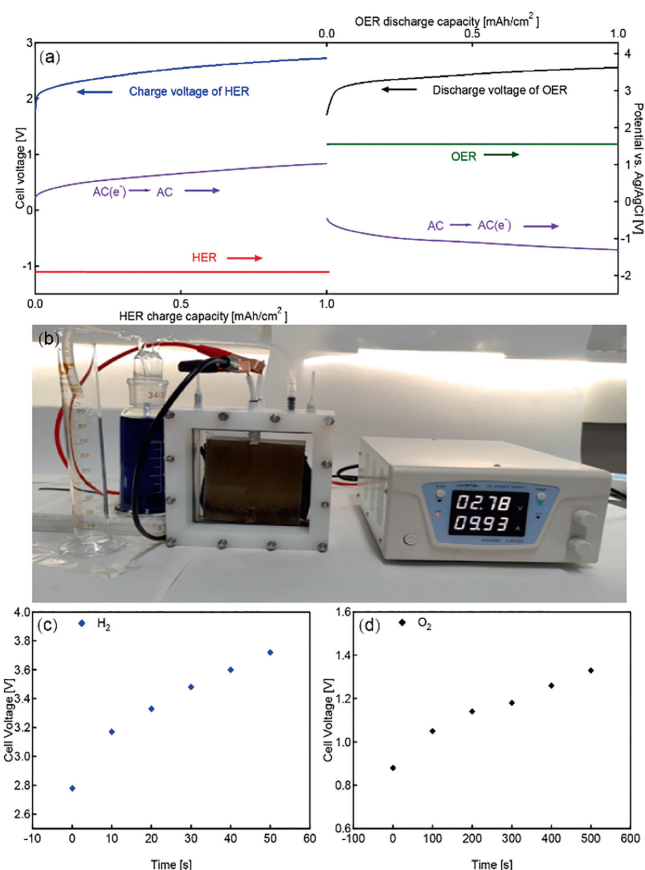


**Fig. 4.** (a) Cell voltage and Potential curves of the hydrogen production (left part) and the oxygen production (right part) at a current of 1 A/cm<sup>2</sup>. (b) The visual configuration of decoupled water electrolysis with NiFe-LDH@Pt-coated Ti-mesh ( $10 \times 10 \text{ cm}^2$ ) and AC relay ( $10 \times 10 \text{ cm}^2$ ). Cell voltage vs. time (above display) for the  $\text{H}_2$  production steps (c) and the  $\text{O}_2$  production steps (d) at a current of 10 A and 1 A respectively.

The selection of proper redox mediators is crucial for decoupled electrolysis. With traditional battery based solid state redox mediators, such as  $\text{NiOOH}/\text{Ni}(\text{OH})_2$ , the long-term stability and current density may not meet the requirements for practical applications. Supercapacitors show much better performances such as charge/discharge rate, specific power, Coulombic efficiency and cycle stability, which is more compatible with unstable green energies, such as solar and wind. Our research may bring some new insights in the selection of proper materials for decoupled electrolysis.

#### Declaration of competing interest

The authors declare that they have no known competing financial interests or personal relationships that could have appeared to influence the work reported in this paper.

#### Acknowledgments

This work was supported by the Shandong Provincial Natural Science Foundation, China (Nos. 2019GSF109029, ZR2021QB190) and was also funded by the National Natural Science Foundation of China (Nos. 21771118, 21701098, 21875128 and 22109077), the Taishan Scholars Climbing Program of Shandong Province (No. tspd20150201), and by the Yantai Double-hundred Talents Project.

## Supplementary materials

Supplementary material associated with this article can be found, in the online version, at doi:10.1016/j.ccl.2022.07.052.

## References

- [1] J. Chen, Y. Tang, S. Wang, et al., *Chin. Chem. Lett.* 33 (2022) 1468–1474.
- [2] X. Cheng, L. Wang, L. Xie, et al., *Chem. Eng. J.* 439 (2022) 135757.
- [3] M. Liu, H. Li, S. Liu, et al., *Nano Res.* 15 (2022) 5946–5952.
- [4] X. Liu, Y. Hou, M. Tang, L. Wang, *Chin. Chem. Lett.* 34 (2023) 107489.
- [5] L. Wang, L. Xie, W. Zhao, S. Liu, Q. Zhao, *Chem. Eng. J.* 405 (2021) 127028.
- [6] S. Wang, L. Wang, L. Xie, et al., *Nano Res.* 15 (2022) 4996–5003.
- [7] L. Xie, L. Wang, W. Zhao, et al., *Nat. Commun.* 12 (2021) 5070.
- [8] M. Guo, A. Qayum, S. Dong, X. Jiao, D. Chen, T. Wang, *J. Mater. Chem. A* 8 (2020) 9239–9247.
- [9] L. Wu, F. Zhang, S. Song, et al., *Adv. Mater.* 34 (2022) e2201774.
- [10] Z.Y. Yu, Y. Duan, X.Y. Feng, et al., *Adv. Mater.* 33 (2021) e2007100.
- [11] F. Liu, C. Shi, X. Guo, et al., *Adv. Sci.* (2022) e2200307.
- [12] C. Zhang, P. Wang, W. Li, et al., *J. Mater. Chem. A* 8 (2020) 19348–19356.
- [13] Z. Cai, P. Wang, J. Zhang, et al., *Adv. Mater.* (2022) e2110696.
- [14] D. Zhou, P. Li, X. Lin, et al., *Chem. Soc. Rev.* 50 (2021) 8790–8817.
- [15] X. Cui, M. Chen, R. Xiong, et al., *J. Mater. Chem. A* 7 (2019) 16501–16507.
- [16] Y. Li, X. Wei, S. Han, L. Chen, J. Shi, *Angew. Chem. Int. Ed.* 60 (2021) 21464–21472.
- [17] T. Wang, L. Tao, X. Zhu, et al., *Nat. Catal.* 5 (2021) 66–73.
- [18] B. You, Y. Sun, *Acc. Chem. Res.* 51 (2018) 1571–1580.
- [19] L.G. Bloor, R. Solaris, K. Bienkowski, et al., *J. Am. Chem. Soc.* 138 (2016) 6707–6710.
- [20] Z. Liu, G. Zhang, K. Zhang, H. Lan, H. Liu, J. Mater. Chem. A 8 (2020) 4073–4082.
- [21] M.D. Symes, L. Cronin, *Nat. Chem.* 5 (2013) 403–409.
- [22] M. Hou, L. Chen, Z. Guo, et al., *Nat. Commun.* 9 (2018) 438.
- [23] W. Ma, C. Xie, X. Wang, et al., *ACS Energy Lett.* 5 (2019) 597–603.
- [24] A.G. Wallace, M.D. Symes, *Joule* 2 (2018) 1390–1395.
- [25] B. Rausch, M.D. Symes, G. Chisholm, L. Cronin, *Science* 345 (2014) 1326–1330.
- [26] L. Chen, X. Dong, Y. Wang, Y. Xia, *Nat. Commun.* 7 (2016) 11741.
- [27] Y. Ma, X. Dong, Y. Wang, Y. Xia, *Angew. Chem. Int. Ed.* 57 (2018) 2904–2908.
- [28] J. Wang, L. Ji, X. Teng, et al., *J. Mater. Chem. A* 7 (2019) 13149–13153.
- [29] Z.P. Ifkovits, J.M. Evans, M.C. Meier, K.M. Papadantonakis, N.S. Lewis, *Energy Environ. Sci.* 14 (2021) 4740–4759.
- [30] P.J. McHugh, A.D. Stergiou, M.D. Symes, *Adv. Energy Mater.* 10 (2020) 2002453.
- [31] J. Huang, Y. Wang, *Cell Rep. Phys. Sci.* 1 (2020) 100138.
- [32] J. Huang, Y. Xie, L. Yan, et al., *Energy Environ. Sci.* 14 (2021) 883–889.
- [33] J. Shang, Q. Huang, L. Wang, et al., *Adv. Mater.* 32 (2020) e1907088.
- [34] Y. Song, Q. Pan, H. Lv, et al., *Angew. Chem. Int. Ed.* 60 (2021) 5718–5722.
- [35] Y. Wang, Y. Song, Y. Xia, *Chem. Soc. Rev.* 45 (2016) 5925–5950.
- [36] A. González, E. Goikolea, J.A. Barrena, R. Mysyk, *Renew. Sustain. Energy Rev.* 58 (2016) 1189–1206.
- [37] Y. Wang, Z. Chen, M. Zhang, et al., *Green Energy Environ.* 7 (2022) 1053–1061.
- [38] Y. Wang, Y. Liu, A. Ejaz, K. Yan, *Chin. Chem. Lett.* (2022), doi:10.1016/j.ccl.2022.05.052.
- [39] M. Guo, L. Wang, J. Zhan, et al., *J. Mater. Chem. A* 8 (2020) 16609–16615.